

A Theoretical and Experimental Study of the Molecular Rearrangement of 5-Methyl-4-nitrobenzofuroxan

Frank Eckert,[†] Guntram Rauhut,^{*,†} Alan R. Katritzky,[‡] and Peter J. Steel[§]

Contribution from the Universität Stuttgart, Institut für Theoretische Chemie, Pfaffenwaldring 55, 70569 Stuttgart, Germany, Florida Center for Heterocyclic Compounds, University of Florida, Department of Chemistry, Gainesville, Florida 32611-7200, and University of Canterbury, Department of Chemistry, Private Bag 4800, Christchurch, New Zealand

Received February 16, 1999. Revised Manuscript Received April 26, 1999

Abstract: The molecular rearrangement of 5-methyl-4-nitrobenzofuroxan to 7-methyl-4-nitrobenzofuroxan was studied by means of ab initio and density functional theory. Experimentally obtained IR spectra and X-ray data support the applicability of the theoretical methods and allow for a complete assignment of the vibrational modes. The influence of the methyl substituent on the underlying tautomeric reaction was investigated in detail. Trends for the reactivity of 4-nitrobenzofuroxans with substituents in the 5-position were established on the basis of an energy partitioning, providing insight into the driving forces of the Boulton–Katritzky rearrangement. Rate constants were calculated for this reaction using different implementations of variational transition-state theory. In addition a reaction yielding 6-methyl-7-nitrobenzofuroxan was investigated as an alternative to the rearrangement considered. An accurate treatment of relative energies of this competing reaction requires very demanding computational methods which could not be applied here. Therefore, energy corrections were estimated from smaller benchmark systems.

2. Introduction

Members of molecular classes of benzofuroxans and benzotriazoles undergo several mono- and bicyclic rearrangements, which are well-recognized for many years even though their mechanistic details are still the subject of current research.^{1,2} This research is partly driven by their pharmacological properties and the importance of these species for biological processes.³ Therefore, comprehensive reviews of benzofurazans and related compounds were published in the recent past.^{4–7}

The Boulton–Katritzky rearrangement (BKR, see Figure 1) of 4-nitrobenzofuroxan, which can be considered as a prototype reaction for a class of molecular rearrangements (see for instance ref 6), was studied quite recently by ab initio and density functional methods.⁸ It was found that the mechanism of this reaction proceeds in one step via a tricyclic, concerted transition state. Since these electron-rich molecules are extremely sensitive to electron-correlation effects, very demanding methods computationally are necessary to yield reliable results for structural

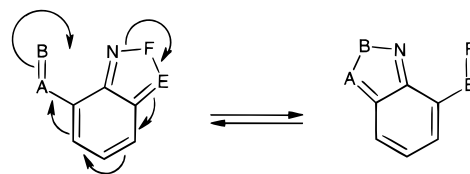


Figure 1. A generalized scheme of the Boulton–Katritzky rearrangement. A,E = N,N⁺–O[–], N⁺–N[–]R, CR; B,F = O,NR,S.

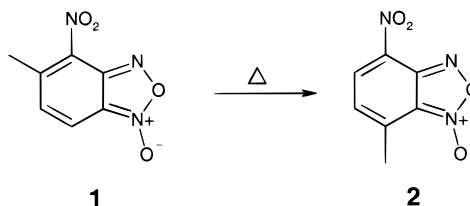


Figure 2. Isomerization of 5-methyl-4-nitrobenzofuroxan **1**.

parameters and energies. Coupled-cluster calculations with a perturbational correction for triple excitations, CCSD(T), based on fourth-order Møller–Plesset geometry optimizations, MP4-(SDQ), lead to a reaction barrier of about 28 kcal/mol after correction for the zero-point vibrational energy. This barrier is too high to be observed by NMR experiments as performed by Harris et al.⁹ However, a substituent in the 5-position dramatically changes the situation. 5-Methyl-4-nitrobenzofuroxan **1** isomerizes to 7-methyl-4-nitrobenzofuroxan **2** upon gentle heating (Figure 2).^{6,10} For substituents other than methyl the 5-isomer can hardly be isolated, and 7-anilino-4-nitrobenzofuroxan rearranges on heating to 5-anilino-4-nitrobenzofuroxan.¹¹ It was assumed at first that the isomerization is controlled by steric hindrance in the 5-isomer. However, the results of Ghosh concerning the retro-BKR¹¹ and those of Takakis et

* To whom correspondence should be addressed. E-mail: rauhut@theochem.uni-stuttgart.de.

[†] University of Stuttgart.

[‡] University of Florida.

[§] University of Canterbury.

(1) Takakis, I. M.; Hadjimihalakis, P. M. *J. Heterocycl. Chem.* **1992**, 29, 121.

(2) Takakis, I. M.; Hadjimihalakis, P. M.; Tsantali, G. G.; Pilini, H. J. *Heterocycl. Chem.* **1992**, 29, 123.

(3) Ghosh, P. B.; Ternai, B.; Whitehouse, M. W. *J. Med. Chem.* **1972**, 15, 1255.

(4) Paton, R. M. 1,2,5-Oxadiazoles. In *Comprehensive Heterocyclic Chemistry II*; Katritzky, A. R., Rees, C. W., Scriven, E. F. V., Eds.; Pergamon Press: New York, 1995; Vol. 4.

(5) Friedrichsen, W., IV. Arenofurazan-1-oxide. In *Houben-Weyl, Methoden der Organischen Chemie*; Schaumann, E., Ed.; Thieme: Stuttgart, 1994; Vol. E8c.

(6) Katritzky, A. R.; Gordeev, M. F. *Heterocycles* **1993**, 35, 483.

(7) Ghosh, P. B.; Ternai, B.; Whitehouse, M. W. *Med. Res. Rev.* **1981**, 1, 159.

(8) Eckert, F.; Rauhut, G. *J. Am. Chem. Soc.* **1998**, 120, 13478.

(9) Harris, R. K.; Katritzky, A. R.; Øksne, S.; Bailey, A. S.; Paterson, W. G. *J. Chem. Soc.* **1963**, 197.

(10) Boulton, A. J.; Katritzky, A. R. *Proc. Chem. Soc.* **1962**, 257.

(11) Ghosh, P. B. *J. Chem. Soc. (B)* **1968**, 334.

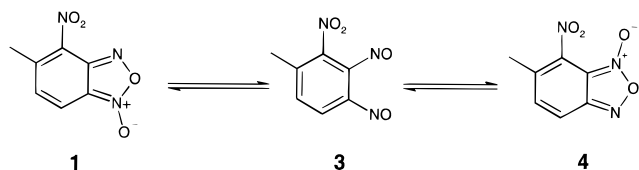


Figure 3. Reaction of 5-methyl-4-nitrobenzofuroxan **1** to 6-methyl-7-nitrobenzofuroxan **4**.

al.^{12,13} on 1,2-alkylenedioxy-nitrobenzofuroxans showed that the direction and exothermicity of the BKR depends on a fine balance of steric, electronic, conformational, and strain effects.⁶ It is thus the intention of this study to investigate the influence of the methyl-substituent on the BKR to gain a general understanding of the driving forces of this reaction.

Moreover, the transition-state barrier of the heterocyclic ring-opening process in benzofuroxans lies well below the barrier of the BKR. Therefore, the alternative reaction toward 6-methyl-7-nitrobenzofuroxan **4** competes in principle with the BKR (see Figure 3). For instance, 6-chloro-7-nitrobenzofuroxan has been observed after photolyzing 5-chloro-4-nitrobenzofuroxan,¹⁴ but in comparison to the educt it is thermodynamically less favorable. The energetics of this reaction mechanism has also been investigated in this study.

3. Experimental Methods

7-Methyl-4-nitrobenzofuroxan, **2**, prepared as described in ref 10 was recrystallized. It has mp 152–163 °C,¹⁰ and the proton NMR agreed with the published data. The infrared spectrum was obtained in mineral oil. X-ray data were collected with a Siemens SMART CCD area detector, using graphite monochromatized Mo K α radiation ($\lambda = 0.71073$ Å). A full sphere of data was collected. The structure was solved by direct methods and refined on F^2 using all data by full-matrix least-squares procedures. Hydrogen atoms were included in calculated positions, with the torsional orientation of the methyl hydrogens deduced from circular Fourier syntheses. A final difference map showed no features greater or less than $0.28 \text{ e} \cdot \text{Å}^{-3}$.

Crystal data for 2 at -115 °C: $C_7H_5N_3O_4$, $M = 195.14$, orthorhombic, space group $Pbca$, $a = 11.2189(12)$ Å, $b = 10.5028(11)$ Å, $c = 13.0799(14)$ Å, $V = 1541.2(3)$ Å³, $Z = 8$, $F(000) = 800$, $D_x = 1.682 \text{ g} \cdot \text{cm}^{-3}$, yellow block, $0.61 \times 0.46 \times 0.38$ mm, $\mu = 0.141 \text{ mm}^{-1}$, $2\theta_{\text{max}} = 53^\circ$, 16 265 reflections collected, 1556 unique reflections ($R_{\text{int}} = 0.020$), 128 parameters, GOF = 1.085, $wR = 0.0873$ for all data, $R = 0.0326$ for 1403 data with $I > 2\sigma(I)$.

4. Computational Methods

Geometries of all structures have been optimized using the hybrid B3-LYP exchange-correlation density functional as implemented in the Gaussian package of ab initio programs.¹⁵ This functional is well-known for its reliable description of geometric parameters and of vibrational spectra in standard molecules. It is even capable of reproducing correctly the endocyclic N–O bond in benzofuroxans. Bonds of this type computed at the Hartree–Fock or second-order perturbational level (MP2) show significant errors in comparison to experimental data, and consequently these methods are not suitable for this class of mol-

ecules.^{16,17} This is caused by unusually strong dynamical electron correlation effects, which are typical for these electron-rich structures. The B3-LYP structures are in very good agreement with MP4(SDQ) geometries as could be shown recently.⁸ We therefore relinquished performing the extremely demanding geometry optimizations at the MP4(SDQ) level in this study. Utilizing the B3-LYP structures coupled-cluster single-point calculations with a perturbational triples correction, CCSD(T), were performed to account for higher correlation effects. A comparatively small 6-31G** basis¹⁸ has been used for most of the calculations presented in this study. However, we were able to show in our previous study⁸ that basis set effects must be considered small. Therefore, to limit the computational effort we used this segmented polarized valence double- ζ basis. Even though a triple- ζ basis would be desirable for treating the O \cdots H interactions more precisely, this was out of the range of feasibility. For the same reason triples corrections in the coupled-cluster calculations were neglected in the investigation of the alternative reaction toward **4** but estimated from smaller benchmark systems. The reliability of this working scheme for the alternative reaction may be questioned because we were able to show⁸ that B3-LYP fails to represent the structure of the transition state of the ring opening of the unsubstituted 4-nitrobenzofuroxan **5** correctly. In analogy one has to expect that the relative energy of transition state **TS2**, which describes the ring opening of **1**, may also be erroneous. However, this problem has little impact on the conclusions of this study. First, such a transition state is not involved in the BKR which is the primary subject of this investigation. Second, an energy correction can be estimated from the relative CCSD//MP4(SDQ) and CCSD//B3-LYP energies as obtained for the corresponding transition state in the reaction of the unsubstituted 4-nitrobenzofuroxan **5**. CCSD and CCSD(T) calculations were carried out using the MOLPRO ab initio program.¹⁹

Vibrational frequencies were computed at the B3-LYP/6-31G* level. Neglecting the polarization functions on hydrogens caused only minor changes in molecular geometries but allowed the use of transferable scaled quantum mechanical (SQM) scaling factors which have been established for this basis only.^{20–22} The SQM scaling procedure uses a set of scaling factors (usually about 10), each of them optimized for scaling force constants belonging to the same class of internal coordinates (i.e. torsions, bendings,...). By correcting for anharmonicity, electron correlation effects, and basis set deficiencies this scheme is significantly superior in comparison to the usual uniform scaling procedure.²³

¹H absolute isotropic shieldings σ were calculated at the GIAO/B3-LYP level using a 6-311G** basis.²⁴ ¹H chemical shifts δ relative to TMS were calculated in ppm from these shieldings according to $\delta = -0.911 \sigma + 29.635$.²⁵ B3-LYP chemical shifts must be considered a compromise between accuracy and computational efficiency as shown by Cheeseman et al.²⁶ Usually B3-LYP chemical shifts are more reliable than Hartree–Fock values but tend to be worse than MP2 ones. However, MP2 is not capable of correctly describing the wave function of benzofuroxans, and therefore GIAO/B3-LYP calculations appear to be the only choice for reliably calculating ¹H chemical shifts of these molecules. NMR calculations were carried out using the PQS program of Pulay et al.²⁷

(16) Rauhut, G. J. *Comput. Chem.* **1996**, *17*, 1848.

(17) Seminario, J. M.; Concha, M. C.; Politzer, P. J. *Comput. Chem.* **1992**, *13*, 177.

(18) Ditchfield, R.; Hehre, W. J.; Pople, J. A. *J. Chem. Phys.* **1971**, *54*, 724.

(19) MOLPRO is a package of ab initio programs written by H.-J. Werner and P. J. Knowles, with contributions from R. D. Amos, A. Berning, D. L. Cooper, M. J. O. Deegan, A. J. Dobbyn, F. Eckert, C. Hampel, T. Leininger, R. Lindh, A. W. Lloyd, W. Meyer, M. E. Mura, A. Nicklass, P. Palmieri, K. Peterson, R. Pitzer, P. Pulay, G. Rauhut, M. Schütz, H. Stoll, A. J. Stone, and T. Thorsteinsson. Version 98.1. University of Birmingham, UK, 1998 (see <http://www.tc.bham.ac.uk/molpro/>).

(20) Rauhut, G.; Pulay, P. J. *Phys. Chem.* **1995**, *99*, 3093.

(21) Rauhut, G.; Pulay, P. J. *Phys. Chem.* **1995**, *99*, 14572.

(22) Baker, J.; Jarzecki, A.; Pulay, P. J. *Phys. Chem. A* **1998**, *102*, 1412.

(23) Scott, A. P.; Radom, L. *J. Phys. Chem.* **1996**, *100*, 16502.

(24) Krishnan, R.; Binkley, J. S.; Seeger, R.; Pople, J. A. *J. Chem. Phys.* **1980**, *72*, 650.

(25) P. Pulay, private communication.

(26) Cheeseman, J.; Tucks, G. W.; Keith, T. A.; Frisch, M. J. *J. Chem. Phys.* **1996**, *104*, 5497.

(12) Takakis, I. M.; Hadjimihalakis, P. M. *J. Heterocycl. Chem.* **1991**, *28*, 1373.

(13) Takakis, I. M.; Hadjimihalakis, P. M.; Tsantali, G. G. *Tetrahedron* **1991**, *47*, 7157.

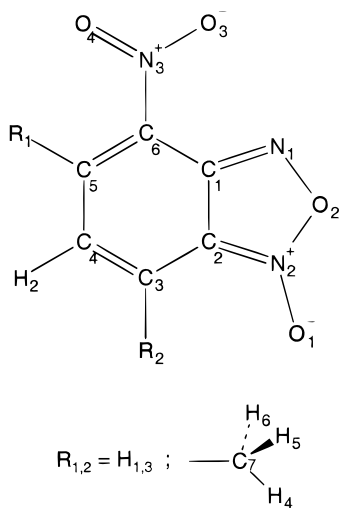
(14) Calzaferrri, G.; Gleiter, R.; Knauer, K.-H.; Martin, H.-D.; Schmidt, E. *Angew. Chem., Int. Ed. Engl.* **1974**, *13*, 52.

(15) Gaussian 94, Revision D.1. Frisch, M. J.; Trucks, G. W.; Schlegel, H. B.; Gill, P. M. W.; Johnson, B. G.; Robb, M. A.; Cheeseman, J. R.; Keith, T.; Petersson, G. A.; Montgomery, J. A.; Raghavachari, K.; Al-Laham, M. A.; Zakrzewski, V. G.; Ortiz, J. V.; Foresman, J. B.; Cioslowski, J.; Stefanov, B. B.; Nanayakkara, A.; Challacombe, M.; Peng, C. Y.; Ayala, P. Y.; Chen, W.; Wong, M. W.; Andres, J. L.; Replogle, E. S.; Gomperts, R.; Martin, R. L.; Fox, D. J.; Binkley, J. S.; Defrees, D. J.; Baker, J.; Stewart, J. P.; Head-Gordon, M.; Gonzalez, C.; Pople, J. A. Gaussian, Inc., Pittsburgh PA, 1995.

Table 1. Experimental (X-ray) and Calculated (B3-LYP/6-31G**) Geometrical Parameters of 5-Methyl-4-nitrobenzofuroxan **1** (C_1) and 7-Methyl-4-nitrobenzofuroxan **2** (Calcd: C_2)

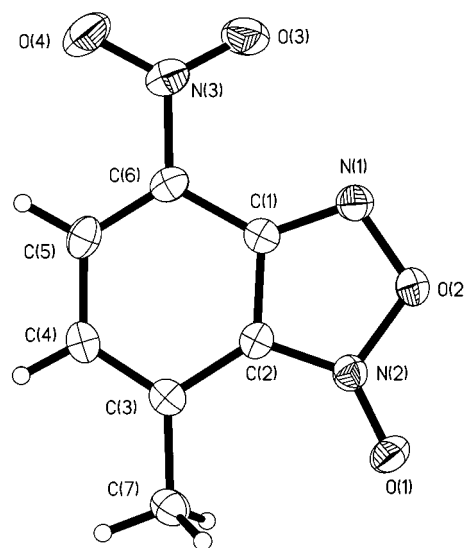
5-methyl-4-nitrobenzofuroxan (1)				7-methyl-4-nitrobenzofuroxan (2)					
r^a	calcd	angle ^a	calcd	r^a	calcd	exptl ^b	angle ^a	calcd	exptl ^b
C ₁ -C ₂	1.424	C ₁ -C ₂ -C ₃	123.6	C ₁ -C ₂	1.431	1.420(2)	C ₁ -C ₂ -C ₃	125.1	125.4(1)
C ₂ -C ₃	1.410	C ₂ -C ₃ -C ₄	116.4	C ₂ -C ₃	1.424	1.427(2)	C ₂ -C ₃ -C ₄	114.6	114.4(1)
C ₃ -C ₄	1.368	C ₃ -C ₄ -C ₅	123.4	C ₃ -C ₄	1.379	1.369(2)	C ₃ -C ₄ -C ₅	122.4	122.6(1)
C ₄ -C ₅	1.444	C ₄ -C ₅ -C ₆	119.1	C ₄ -C ₅	1.425	1.426(2)	C ₄ -C ₅ -C ₆	122.4	122.2(1)
C ₅ -C ₆	1.384	C ₅ -C ₆ -C ₁	119.9	C ₅ -C ₆	1.371	1.359(2)	C ₅ -C ₆ -C ₁	118.7	119.2(1)
C ₆ -C ₁	1.439	C ₆ -C ₁ -C ₂	117.5	C ₆ -C ₁	1.435	1.436(2)	C ₆ -C ₁ -C ₂	116.7	116.3(1)
C ₁ -N ₁	1.325	C ₂ -N ₂ -O ₁	134.4	C ₁ -N ₁	1.324	1.327(2)	C ₂ -N ₂ -O ₁	134.7	135.5(1)
C ₂ -N ₂	1.345	C ₂ -N ₂ -O ₂	105.5	C ₂ -N ₂	1.347	1.338(2)	C ₂ -N ₂ -O ₂	106.0	106.5(1)
N ₁ -O ₂	1.376	N ₁ -O ₂ -N ₂	110.2	N ₁ -O ₂	1.375	1.383(1)	N ₁ -O ₂ -N ₂	110.3	109.5(1)
N ₂ -O ₂	1.436	N ₁ -C ₁ -C ₂	111.4	N ₂ -O ₂	1.432	1.440(1)	N ₁ -C ₁ -C ₂	111.6	112.4(1)
N ₂ -O ₁	1.221	C ₁ -N ₁ -O ₂	105.6	N ₂ -O ₁	1.223	1.232(1)	C ₁ -N ₁ -O ₂	105.5	105.1(1)
C ₆ -N ₃	1.462	C ₆ -N ₃ -O ₃	116.9	C ₆ -N ₃	1.458	1.454(2)	C ₆ -N ₃ -O ₃	116.9	117.7(1)
N ₃ -O ₃	1.228	C ₆ -N ₃ -O ₄	118.1	N ₃ -O ₃	1.229	1.227(2)	C ₆ -N ₃ -O ₄	117.8	118.1(1)
N ₃ -O ₄	1.234	C ₂ -C ₃ -H ₁	120.7	N ₃ -O ₄	1.233	1.228(2)	C ₂ -C ₃ -C ₇	121.8	121.0(1)
C ₃ -H ₁	1.084	C ₃ -C ₄ -H ₂	119.4	C ₃ -C ₇	1.502	1.499(2)	C ₃ -C ₄ -H ₂	119.3	
C ₄ -H ₂	1.083	C ₆ -C ₅ -C ₇	124.2	C ₄ -H ₂	1.085		C ₆ -C ₅ -H ₃	117.6	
C ₅ -C ₇	1.509	C ₅ -C ₇ -H ₄	110.5	C ₅ -H ₃	1.084		C ₃ -C ₇ -H ₄	111.1	
C ₇ -H ₄	1.094	C ₅ -C ₇ -H ₅	112.3	C ₇ -H ₄	1.096		C ₃ -C ₇ -H ₆	110.5	
C ₇ -H ₅	1.091	C ₅ -C ₇ -H ₇	109.8	C ₇ -H ₅	1.096		H ₄ -C ₇ -H ₅	106.3	
C ₇ -H ₆	1.092	H ₄ -C ₇ -H ₅	106.2	C ₇ -H ₆	1.093		H ₄ -C ₇ -H ₆	108.1	
		H ₄ -C ₇ -H ₆	108.7				H ₄ -C ₇ -C ₃ -C ₂	59.1	
		O ₃ -N ₃ -C ₆ -C ₁	25.9				C ₅ -C ₆ -N ₃ -O ₄	0.0	10.9(2)
		H ₄ -C ₇ -C ₅ -C ₄	103.2						
		H ₅ -C ₇ -C ₅ -C ₄	-138.4						
		H ₆ -C ₇ -C ₅ -C ₄	-16.6						

^a Bond lengths are in Ångströms and angles in degrees. ^b Estimated standard deviations for experimental values are given in parentheses.

**Figure 4.** The atomic labeling of 5/7-methyl-4-nitrobenzofuroxan.

5. Geometries/Structures: Experimental and Theoretical Results

Experimental and computed geometric parameters for **1** and **2** are shown in Table 1. The labeling of the atoms is given in Figure 4. The agreement between theory and experiment is excellent, even for the critical N₂-O₂ bond which is known for its sensitivity to the computational method (see refs 8, 16). The structure of **2** in the solid state was determined by single-crystal X-ray crystallography at -115 °C. The geometry within the benzofuroxan group is similar to that in previously reported structures containing this ring system.²⁸ Figure 5 shows a thermal ellipsoid plot of the structure, which has the plane of the nitro-group twisted out of the attached six-membered ring by 11.0(1)°. This distortion is not observed in the computed

**Figure 5.** Thermal ellipsoid plot of the X-ray crystal structure of **2**.

structure which shows C_s symmetry. We believe that this slight deviation from coplanarity of the nitro-group in the solid state is due to intermolecular packing interactions, as the nitro-group oxygen atoms show a number of relatively short contacts to hydrogen atoms of adjacent molecules (see Figure 6). This is supported by the results of Prout et al.²⁹ for 4,6-dinitrobenzofuroxan. They report a dihedral angle of only 2.7° between the nitro-group in the ortho position to the furoxan ring and the six-membered ring. Note, the relative arrangement of the molecules in the crystal is less complex for 4,6-dinitrobenzofuroxan than for **2** which results in fewer short contacts. Differences between **1** and **2** in the geometric parameters of the furoxan ring are marginal and account for less than 0.004 Å and 0.5°. Moreover, they are more pronounced in the ortho-

(27) Wolinski, K.; Hinton, J. F.; Pulay, P. *J. Am. Chem. Soc.* **1990**, *112*, 8251.

(28) Britton, D. *Acta Crystallogr., Sect. C* **1992**, *48*, 1248.

(29) Prout, C.; Hodder, O.; Viterbo, D. *Acta Crystallogr., Sect. B* **1972**, *28*, 1523.

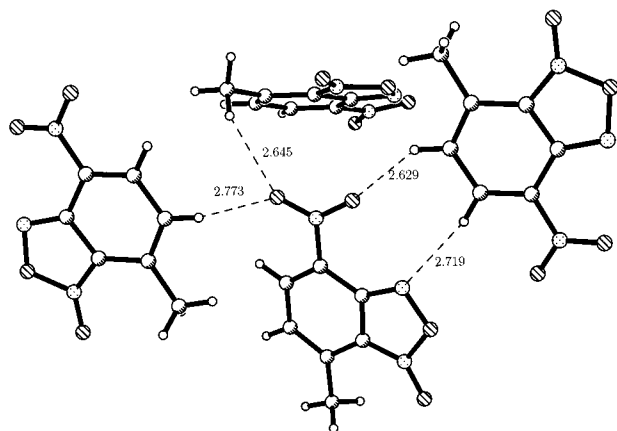


Figure 6. Intermolecular contacts in the unit cell of **2**. Distances in [Å].

quinonoid six-membered ring system. Bond alternation appears to be more strongly emphasized in **1** than in **2**. Furthermore, the double bond in direct vicinity of the methyl substituent is slightly longer than the other, i.e., in **1** C₃–C₄ is shorter than C₅–C₆, while the opposite can be seen for **2**. This strong bond alternation distinguishes the studied system clearly from doubly substituted benzenes (for instance *o*-nitrotoluene) which are less sensitive with respect to substituents in ortho position.

As can be seen from Table 1 for structure **1**, the interaction of the methyl-group with the nitro-group leads to an out-of-plane deformation of the latter. This effect will be discussed in detail below. Structure **2** allows for two different conformations in C_s symmetry: a staggered conformer, in which the atom H₆ points away from the exocyclic O₁, and an eclipsed conformer, in which the H₆ points toward the exocyclic O₁. Since the distance between the nearest hydrogen atom and the exocyclic oxygen is significantly shorter (by about 0.5 Å) in the eclipsed conformer one may expect a stronger stabilizing interaction for this structure. However, this is not the case as can be explained from the shape of the O···H potential. Since the acidity of the methyl-hydrogens is comparatively low, the potential curve shows a shallow minimum at larger distances and already becomes repulsive at the distance of 2.346 Å, i.e., the O···H distance in the eclipsed conformer. At the distance of 2.825 Å (i.e., the O···H distance in the staggered conformer) the potential is attractive and therefore the eclipsed conformer is destabilized by about 1 kcal/mol. Frequency calculations showed that the eclipsed conformer represents the transition state of the methyl rotation in **2**. This is in agreement with our X-ray results which clearly show the staggered conformer as determined from Fourier maps.

Note that, while the tricyclic transition state of the unsubstituted 4-nitrobenzofuroxan **5** is of C_{2v} symmetry and thus shows identical bond lengths for the breaking and the new bond,⁸ this of course cannot be found for the transition state of the methylated compounds. Here, the interaction with the methyl group causes a difference of about 0.025 Å between the two bonds under consideration. The C_s structure of the transition state is given in Figure 7. In comparison to the transition state of 4-nitrobenzofuroxan the bond mainly affected by the methyl-group is the C₅–C₆ bond of the six-membered ring. Due to the interaction of the methyl-group with the nitro-group this bond is 0.016 Å longer in the methylated compound. Since **TS1** is planar in structure, the rotation of the nitro-group and the methyl-group of the asymmetrical educt **1** must characterize the very first part of the reaction.

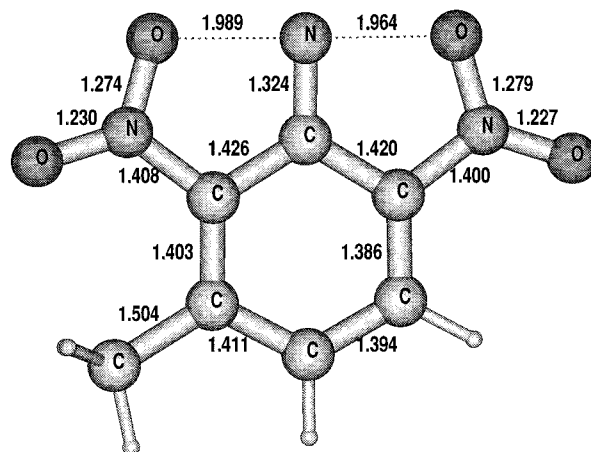


Figure 7. Structure and bond lengths of transition state **TS1** occurring in the molecular rearrangement of 5-methyl-4-nitrobenzofuroxan **1** (B3-LYP/6-31G**).

Table 2. Relative Energies^a (6-31G**) of Structures Involved in the BKR of 5-Methyl-4-nitrobenzofuroxan **1**^b

energy	geometry	TS1		2	
		<i>E</i> _{rel}	<i>E</i> _{rel} ^{scal}	<i>E</i> _{rel}	<i>E</i> _{rel} ^{scal}
B3-LYP	B3-LYP	20.67	19.73	-4.34	-4.41
CCSD	B3-LYP	28.29	27.35	-3.77	-3.82
CCSD(T)	B3-LYP	26.36	25.41	-3.68	-3.62

^a *E*_{rel}: Energies relative to structure **1** in [kcal/mol], not corrected for zero-point vibrational energies. *E*_{rel}^{scal}: Energies relative to structure **1** in [kcal/mol], corrected by scaled ZPEs, scaling factors taken to be 0.963 for B3-LYP. CCSD and CCSD(T) energies have been corrected by scaled B3-LYP ZPEs. ^b Absolute energies and zero-point vibrational energies (ZPE) for all calculations presented in this table are provided in the Supporting Information.

6. Energetics

As previously discussed,⁸ the most likely reaction path for this isomerization is a one-step process via a tricyclic transition state **TS1**. Relative energies for this reaction path are given in Table 2. In comparison to the rearrangement of the unsubstituted 4-nitrobenzofuroxan **5** the transition state of the BKR for the methylated compound **1** is lowered by 2 kcal/mol. The reaction energy is about -4 kcal/mol at the CCSD(T) level, which can be regarded as the most accurate. These values readily explain why **1** isomerizes upon gentle heating while the unsubstituted compound does not. Since entropy and temperature corrections are extremely small (about 0.5 kcal/mol for the reaction barrier at 298 K, i.e., 2%), Gibbs free energies are essentially identical with the zero-point energy corrected relative energies as provided in Table 2. The problem remaining to be solved is to analyze the origin of the energy-lowering of the 7-methyl compound in comparison to that of the 5-isomer, i.e., to identify the driving forces of the BKR.

A difficulty must be acknowledged in defining the nature of these driving forces. It is not possible, for example, to separate inductive electronic effects from mesomeric electronic effects or hyperconjugation simply by computing relative energies. Even though we address certain energy contributions to specific interactions in this study, most of these computed quantities rely on some a priori approximations and can thus be questioned. Most of these assumptions are due to the problem that all of the relevant interactions are intramolecular and not intermolecular. Therefore, most numbers presented in this work must be considered estimates rather than exact values. However, they are accurate enough to allow for a qualitative interpretation to gain a deeper understanding of this reaction.

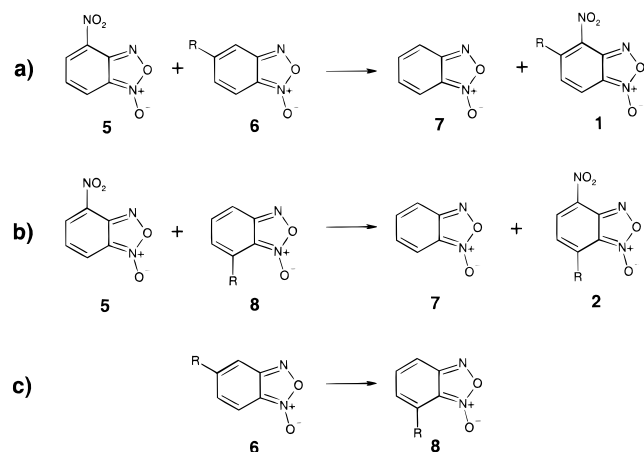


Figure 8. Isodesmic reactions as used for calculating intramolecular interaction energies.

Table 3. Interaction Energies [kcal/mol] (6-31G*) for Different Substituents R Calculated from Isodesmic Reactions

R	method	ΔE_o^a	ΔE_p^a	$\Delta E_{5/7}^a$	ΔE_{BKR}^a
CH ₃	B3-LYP	2.80	-0.88	-0.72	-4.37
	CCSD	2.14	-0.70	-1.04	-3.88
F	B3-LYP	6.29	0.02	4.11	-2.15
	CCSD	6.42	0.37	4.91	-1.14
Cl	B3-LYP	7.94	0.60	2.88	-4.46
CN	B3-LYP	7.62	2.57	1.89	-3.16
CHO	B3-LYP	7.21	2.17	1.46	-3.58

^a For a definition of the interaction energies see text and Figure 8. Absolute energies for all calculations presented in this table are provided in the Supporting Information.

6.1. Isodesmic Reactions. Energy partitioning for intramolecular reactions by using quantum chemical calculations is very limited. We have used a set of isodesmic reactions, whose reaction energies represent the interaction energies between the methyl-group, the nitro-group, and the furoxan ring. The isodesmic reactions used here are depicted in Figure 8. Reaction **a** in Figure 8 provides the ortho-interaction energy (ΔE_o) between the methyl-group in the 5-position and the nitro-group. Correspondingly, the para-interaction (ΔE_p) between the methyl-group in the 7-position and the nitro-group is given by reaction **b**. The interaction between the methyl-group and the furoxan-ring cannot be computed directly, but the difference ($\Delta E_{5/7}$) between the interactions energies of the furoxan-ring with the methyl-group in 5-position and in 7-position can be calculated from reaction **c**. Note that, the reaction energy (ΔE_{BKR}) of the tautomeric rearrangement of **1** is directly given by

$$\Delta E_{BKR} = -\Delta E_o + \Delta E_p + \Delta E_{5/7}$$

Schemes such as those in Figure 8 were extensively used for calculating substituent interactions in polysubstituted benzenes.³⁰ Interaction energies calculated from these reactions do not, of course, give absolute values, but relative ones which refer to the corresponding interactions of the substituents with hydrogen atoms.

Interaction energies were computed for a small set of different substituents and are shown in Table 3. For the methyl and the fluorine substituents these energies were calculated using both the B3-LYP functional and the coupled-cluster approach. A comparison shows that the percentage error can be large, but absolute errors do not exceed 1 kcal/mol. Due to the deficiency of the B3-LYP functional in assessing dispersion energies the

DFT calculations must be considered with care. Still, the numbers presented in Table 3 demonstrate that one might not expect qualitative changes in the interpretation of these energies for high-order quantum chemical methods.

Therefore, we have focused our attention on the B3-LYP data, which are significantly cheaper to obtain. For the discussion below it is of importance to emphasize that these energies were obtained from fully relaxed structures. In terms of steric effects, strain effects, etc. the computed interaction energies do not provide any information about their nature, except their sign, which denotes the interaction to be stabilizing or destabilizing, respectively. As can be seen from Table 3 the bicyclic BKR is not solely driven by the interaction of the nitro-group and the methyl-group in the 5-position (ΔE_o). Although the ΔE_o contribution dominates, the interactions of the substituents with the furoxan ring play a significant role, especially when the substituent allows for mesomeric effects. The methyl-substituent differs from most other groups by stabilizing ΔE_p and $\Delta E_{5/7}$ contributions and a comparably weak, repulsive interaction between the nitro-group and the methyl-substituent in ortho-position.

To gain more insight into the nature of these interactions, the dominating ortho-contribution has been investigated more closely by introducing constraints into the isodesmic reactions. The enhanced bond alternation in **1** and the distortion of the nitro-group suggest that strain and steric effects are of significant importance. To separate these effects from simple electrostatic through-space interactions of the methyl-group with its neighboring nitro-group we have recalculated isodesmic reaction **a** by freezing the atoms of all four structures to the geometry of **1**. This procedure of course does not cover the position of the hydrogen atoms which replace the methyl- or nitro-groups. Although tests showed that the exact position of the hydrogens is of minor importance ($\Delta E \approx 0.1$ kcal/mol) we have used the bond length and bond angle of the hydrogen in the 4-position to be the same as in the fully relaxed 5-methylbenzofuroxan **6** on both sides of the isodesmic reaction. Analogously, the position of the hydrogen in the 5-position has been taken from the relaxed structure of 4-nitrobenzofuroxan **5**. Using this scheme one obtains an interaction energy of 0.2 kcal/mol for the O...H through space interaction.

Tests using larger triple- ζ bases showed that this value does not change significantly upon variation of the basis set. These results demonstrate that the contribution of a repulsive through-space interaction between the nitro- and the methyl-group amounts to less than 10% of the total destabilizing ortho-interaction (ΔE_o).

6.2. Rotational Barriers. Further insight into the ortho-interaction can be gained from a study of the barrier to rotation of the nitro-group. Figure 9 shows the energy profile upon rotation of this group in **1** and **5** (left-hand side) and the analogous profiles of the corresponding fluoro-compounds (right-hand side). As discussed above, the neglect of dispersion energy at the B3-LYP level of theory³¹ might lead to errors in the rotational potential. However, it can be argued from recent CASSCF calculations on the corresponding barrier in nitrobenzene³² (reported to be 4.7 kcal/mol) that the hindered rotation in **5** found to be 6.0 kcal/mol seems reasonable; i.e., again the B3-LYP calculations results remain applicable in this case. This finding is in agreement with a study of Oie et al.,³³ who showed that rotational barriers are reliably described by most DFT

(31) Kristyan, S.; Pulay, P. *Chem. Phys. Lett.* **1994**, 229, 175.

(32) Takezaki, M.; Hirota, N.; Terazima, M.; Sato, H.; Nakajima, T.; Kato, S. *J. Phys. Chem.* **1997**, 101, 5190.

(33) Oie, T.; Topol, I. A.; Burt, S. K. *J. Chem. Phys.* **1995**, 99, 905.

(30) Pross, A.; Radom, L. *Prog. Phys. Org. Chem.* **1981**, 13, 1.

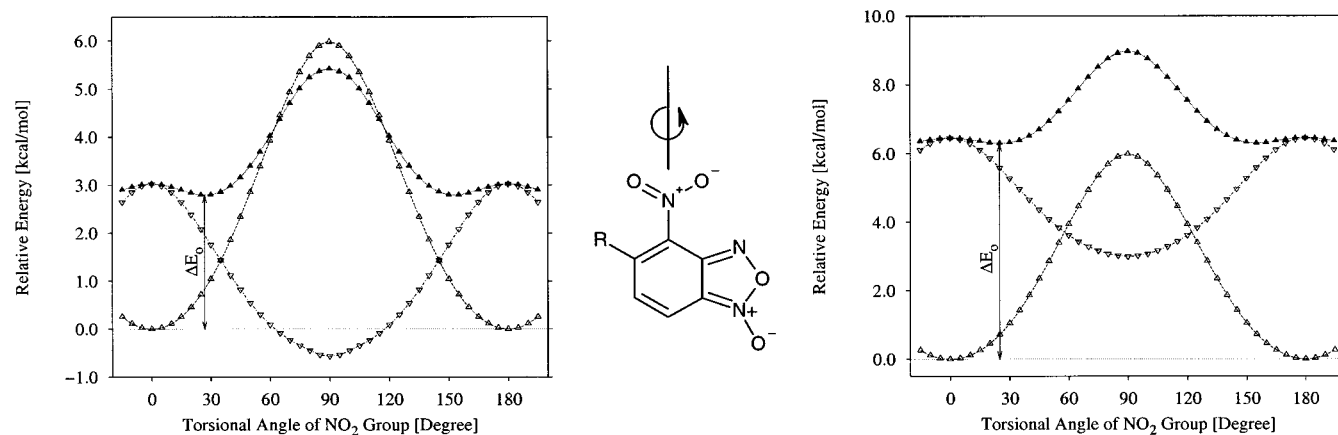


Figure 9. Energy profile of the rotation of the nitro-group in 5-methyl-4-nitrobenzofuroxan **1** and 4-nitrobenzofuroxan **5** (left-hand side) and their fluorinated analogues (right-hand side). (Δ) rotational energy profile of the nitro group in **5**, (\blacktriangle) rotational energy profile of nitro-group in **1**, (∇) energy difference between \blacktriangle and Δ .

functionals, although the B3-LYP functional was not included in their investigation. Figure 9 shows that the potential of **1** (\blacktriangle) beyond a distortion of about 40° appears to be exclusively dominated by the rotation of the nitro-group while in the region below this value other contributions may also overcompensate this particular one as well. The structure at the energetic minimum of **1** shows a torsional angle of 26.9° for the nitro-group as marked in Figure 9. Assuming simple additivity of the energetic contributions one can compute an energy contribution of 0.8 kcal/mol for a distortion of 26.9° from the rotational profile in **5**. Table 5 summarizes the torsional angles of the nitro-group relative to the ring plane for a set of substituents. A comparison of the data for the methyl and the fluorine substituent (which both essentially cause the rotation of the nitro-group by about 26°) shows that the exothermicity of the molecular rearrangement (ΔE_{BKR}) cannot directly be related to the distortion of the nitro-group, nor can ΔE_o be related to the torsional angle or vice versa. The relative energy contributions (given in Table 5 in %) arising from the out-of-plane rotation of the nitro-group vary even though the torsional angle is in the same range. The same effect can be seen for the methoxy- and the formyl-substituents. However, for very bulky substituents (see the sequence F, Cl, and Br) the rotation becomes the dominant contribution and thus dominates the exothermicity of the reaction as well. The nature of the out-of-plane distortion, of course, is well understood: Repulsive, electrostatic interactions between the nitro-group and the methyl-substituent in the ortho-position can be compensated by an out-of-plane rotation of the nitro-group, which consequently leads to decreased conjugation of the π -system of the nitro-group with that of the ring systems. Therefore, in the following we simply will call the destabilizing energy contribution caused by poor conjugation the *anti-conjugative contribution*. Thus, although the distortion of the nitro-group must be considered a driving force for the BKR, it originates from repulsive interactions between the methyl- and nitro-group in ortho-position. In the framework of chemical terminology this interaction must be considered to be steric.

Table 5 also shows the reaction barriers, ΔE^\ddagger , of the BKR of 5-R-substituted nitrobenzofuroxans. Since these data refer to B3-LYP calculations, they must be considered too low (see above and ref 8). However, relative changes in the barrier between different substituents are less sensitive to the level of theory and thus the data provided in Table 5 demonstrate the variation of the activation energy in dependence on the substituent. A simple correlation between the reaction energies,

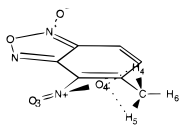
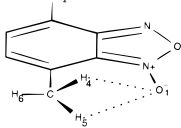
ΔE_{BKR} , and the activation barrier, ΔE^\ddagger , cannot be deduced from this limited set of data, i.e., the occurrence of early or late transition states within these BKR must be expected to be a complex function of several electronic effects. Interestingly, a common structural element of all transition states investigated here is the coplanarity of the nitro-group with the six-membered ring and consequently a mirror plane can be found for all structures, even though the educts may be strongly distorted. This indicates, that this coplanarity is an essential prerequisite which provides insight into the orbitals involved in the reaction.

6.3. O \cdots H Interactions and Strain Effects. Subtracting the anti-conjugative contribution from the rotational profile of **1** yields a potential that is also displayed in Figure 9 and denoted by (∇). This potential represents the ortho-interaction between the methyl- and the nitro-group caused by other than anti-conjugative effects. The interaction is repulsive at the equilibrium structure of **1** but attractive at a distortion between 60 and 120° . By contrast, the corresponding potential of the fluorinated compound remains repulsive instead. From the constrained isodesmic reactions one knows that the O \cdots H interaction at the equilibrium structure is repulsive by about 0.2 kcal/mol only and thus cannot account for the 2.0 kcal/mol destabilization energy which remains after subtracting the anti-conjugative contribution from ΔE_o . Therefore, other destabilizing contributions must dominate the ortho-interaction.

We consider another dominant contribution of these remaining effects to be strain effects in the ring systems, i.e., effects due to the strongly pronounced bond alternation in the six-membered ring of the equilibrium structure of **1**. In a manner similar to that described above we have estimated this contribution from calculations on structures with fixed geometric parameters. We froze the ring systems of **1** and **2** as obtained for their relaxed geometries and substituted the methyl- and nitro-groups by hydrogens as described above. This formally yields **7** on both sides of the reaction, but the geometric parameters differ according to the parameters in **1** and **2**. This scheme allows to compute strain effects in **1** relative to **2**. The destabilization energy obtained this way accounts for 0.6 kcal/mol and thus appears to be as important as the anti-conjugative contribution.

However, although this contribution may change upon rotation of the nitro-group, it cannot readily explain the attractive potential between 60 and 120° . Yet, the shape of this potential can be understood based on the O \cdots H interactions. Table 4 summarizes some properties related to the O \cdots H moiety in the equilibrium structures of **1** and **2**. A simulation of the ^1H NMR spectrum at the GIAO/B3-LYP/6-311G** level of theory shows

Table 4. Comparison of the O...H Interactions in 5-Methyl-4-nitrobenzofuroxan and 7-Methyl-4-nitrobenzofuroxan^a

	5-Methyl-4-nitrobenzofuroxan	7-Methyl-4-nitrobenzofuroxan
		
distances	O ₄ -H ₄ : 2.629 O ₄ -H ₅ : 2.415	O ₁ -H ₄ : 2.825 O ₁ -H ₅ : 2.825
mulliken charges	C ₇ : -0.358 H ₄ : 0.164 H ₅ : 0.151 H ₆ : 0.112	C ₇ : -0.371 H ₄ : 0.155 H ₅ : 0.155 H ₆ : 0.124
¹ H chemical shifts	H ₄ : 3.50 H ₅ : 3.22 H ₆ : 2.44	H ₄ : 3.16 H ₅ : 3.16 H ₆ : 2.56

^a Bond lengths in Å. Chemical shifts in ppm. See text for computational details.

Table 5. Influence of Substituents R on the Distortion of the Nitro-Group in 5-R-4-nitrobenzofuroxan; R = Methyl, Trifluoromethyl, Methoxy, Formyl, Cyano, Fluoro, Chloro, Bromo^a

R	Θ	ΔE _{BKR}	E _{rot}	%E _{rot} ^{BKR}	%E _{rot} ^o	ΔE [‡]
CH ₃	26.9	-4.4	-0.8	19.2	28.6	19.7
CF ₃ ^b	52.2	-5.2	-3.1	59.3		21.6
OCH ₃ ^b	35.6	-6.5	-1.5	23.1		19.0
CHO	36.4	-3.6	-1.5	42.0	20.8	22.5
CN	0.0	-3.2	0.0	0.0	0.0	22.2
F	24.9	-2.2	-0.7	33.2	11.1	22.5
Cl	47.1	-4.5	-2.2	49.4	28.9	21.1
Br ^c	54.9	-4.8	-3.4	70.0		20.7

^a Θ: Rotational angle in deg. ΔE_{BKR}: Reaction energy at the B3-LYP/6-31G* level kcal/mol. E_{rot}: Contribution of the anti-conjugative effect to ΔE_{BKR} in kcal/mol. %E_{rot}^{BKR}: Relative contribution of the anti-conjugative effect to the reaction energy in %. %E_{rot}^o: Relative contribution of the anti-conjugative effect to ΔE_o in %. ΔE[‡]: B3-LYP/6-31G* Reaction barrier in kcal/mol. Note, due to the systematic error of the B3-LYP functional these barriers are consistently too low (compare Table 2). Absolute energies for all calculations presented in this table are provided in the Supporting Information. ^b Θ, ΔE[‡], and ΔE_{BKR} refer to a 6-31G** basis. ^c Utilizing a pseudopotential for the Br atom taken from ref 62.

that the signal of the two interacting hydrogens is shifted by about 0.5–1.0 ppm. In agreement with our discussion above, this indicates nonnegligible interactions with the nitro-group in **1** and the exocyclic oxygen in **2**. However, this shift does not allow denoting the interacting potential as attractive or repulsive. The most obvious difference between the two structures under consideration is the O...H distance. In **2** the distance is considerably larger than in **1**, and thus the same argumentation holds true as used in the geometry section: in **1** the O...H distance is too short, and thus the corresponding potential is repulsive by about 0.2 kcal/mol. On the contrary, at a distance of 2.825 Å in **2** the potential is attractive which is able to explain the negative contribution of ΔE_{5,7}. The same effect can be seen when rotating the nitro-group in **1**. In the equilibrium structure of **1** two O...H distances are below 2.7 Å, while in the attractive range of the potential three O...H distances in the range between 2.7 and 3.5 Å can be found.

Consequently, the stabilizing O...H interaction competes with the destabilizing anti-conjugative effect. Therefore, the torsional angle of the nitro-group in **1** is predominantly defined by the equilibrium of these two interactions. In the case of the potential of 5-fluoro-4-nitrobenzofuroxan (see Figure 9) the interaction

remains repulsive upon rotation of the nitro-group but becomes less stabilizing as the O...F distances increase.

When all of the different contributions of the ortho-interaction discussed above are summed, they do not account for the total magnitude of ΔE_o. This of course must be expected since the applied energy partitioning is able to quantize only some major contributions and cannot account for the entirety of all effects. For instance, the rotation of the methyl-group, which is coupled to the rotation of the nitro-group, will certainly contribute to the destabilization (the rotational barrier of this group in **6** is about 1.0 kcal/mol), but its contribution to ΔE_o is difficult to estimate. Furthermore, the approximative nature of our calculations and the assumption of pure additivity of the energy contributions introduces additional conceptual errors.

6.4. Inductive Effects and Hyperconjugation. Unfortunately, the discussion given above is not able to explain the stabilizing interaction of the methyl-substituent with the nitro-group in the para-position as occurring in **2**. Although this cannot be proven by means of an energy-partitioning, we explain this stabilization by the inductive effect of the methyl-group and perhaps hyperconjugation. A very similar contribution has been found by Hehre et al.³⁴ for the interaction of a nitro-group with a methyl-substituent in *p*-nitrotoluene. Assuming an inductive contribution of about -0.9 kcal/mol for the para-interaction one would at least estimate a similar contribution for the ortho-interaction. However, we consider the computed strain and anti-conjugative effects responses to an initial repulsive interaction with the nitro-group still lying in the ring plane. This initial repulsion of course is partly compensated by the inductive effect of the methyl group, and thus the computed contributions are responses to initial repulsive *plus* stabilizing inductive and hyperconjugative effects. Consequently, the rotational profile shown in Figure 9 is already corrected for this stabilizing contribution, which due to its σ-character has only little impact on the shape of the barrier. In a purely hypothetical consideration a neglect of these contributions would shift the whole profile to higher values but would also lead to stronger strain effects and a larger out-of-plane distortion of the nitro-group. This readily explains the comparably small value of ΔE_o and the relatively small torsional angle.

7. Vibrational Spectra: Experimental and Theoretical Results

Theoretical predictions of the vibrational spectra of **1** and **2**, together with a normal coordinate analysis, was performed using the SQM technique.^{35–37} Relative to the commonly used uniform scaling of vibrational frequencies this method results in significantly improved spectra. We were able to show that this procedure is mandatory for benzofuroxans which require a correction not only of the vibrational frequencies but also of their intensities. For instance, the intensities of the two characteristic bands at about 1600 cm⁻¹ are quite sensitive to scaling, i.e., the normal modes change upon the applied scaling of the force constants. The scaling factors used here are taken from the set of transferable scaling factors which were obtained

(34) Hehre, W. J.; Radom, L.; Schleyer, P. v. R.; Pople, J. A. *Ab Initio Molecular Orbital Theory*; John Wiley & Sons: New York, 1986.

(35) Fogarasi, G.; Pulay, P. *Ab Initio Calculation of Force Fields and Vibrational Spectra*. In *Vibrational Spectra and Structure*; Durig, J. R., Ed.; Elsevier: Amsterdam, 1985; Vol. 14.

(36) Pulay, P.; Fogarasi, G.; Pongor, G.; Boggs, J. E.; Vargha, A. *J. Am. Chem. Soc.* **1983**, *105*, 7037.

(37) Pulay, P.; Zhou, X.; Fogarasi, G. Development of an *Ab Initio* Based Database on Vibrational Force Fields for Organic Molecules. In *Recent Experimental and Computational Advances in Molecular Spectroscopy*; Fausto, R., Ed.; Kluwer: Dordrecht, 1993.

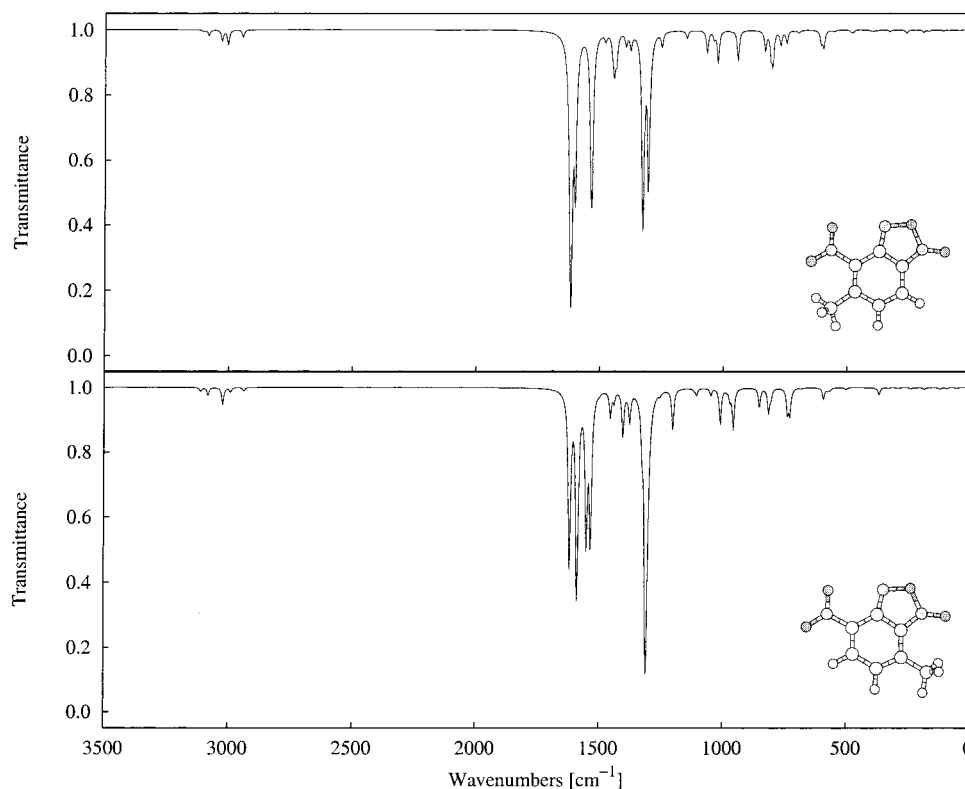


Figure 10. Calculated (SQM/B3-LYP/6-31G*) IR vibrational spectra of 5-methyl-4-nitrobenzofuroxan **1** and 7-methyl-4-nitrobenzofuroxan **2**.

from a database of 347 vibrational frequencies (for details see refs 20, 38³⁸). These factors were proven to be reliable for most organic molecules containing common structural motifs. However, due to the unusual structure of the furoxan ring we found it necessary to reoptimize the scaling factors for N–O stretchings for **1** and **2** as has been done recently for the investigation of the IR spectrum of benzofuroxan.³⁸ The previously used factor of 0.890 was extended into two factors, the first one (0.880) adjusted to exocyclic NO stretchings and the second (0.901) to endocyclic NO stretchings. Tests on the experimentally well-known spectra of benzofuroxan and nitrobenzene showed that this differentiation indeed leads to a significant improvement. The natural internal coordinates generated for **2** and their corresponding scaling factors as used in the scaling procedure are provided in the Supporting Information.

The calculated spectra of **1** and **2** are shown in Figure 10 and the assignment of all fundamentals of **2** are given in Table 6 (the complete assignment of **1** is provided in the Supporting Information). The computationally predicted spectrum of 7-methyl-4-nitrobenzofuroxan **2** agrees nicely with our measured spectrum. Bands associated with deformations of the methyl group show slightly larger deviations than others. This must be expected, since the interaction between the exocyclic oxygen and the hydrogens of the methyl group leads to a shift of these bands, while the applied scaling factor refers to free rotating methyl groups. The intensity of the NO₂ stretchings at 1307 cm⁻¹ is remarkably high. Unfortunately, our experimental spectrum does not support the finding that this vibration is the dominant band of the spectrum. The corresponding vibration in the SQM spectrum of **1** shows significantly lower intensity but strong coupling with an in-plane ring deformation. We address this to the anti-conjugative effects found in this structure and the coupled strain effects of the ring system. The positions of the symmetrical NO stretching bands in **1** and **5** differ by

about 17 cm⁻¹, in agreement with the general finding that an increased symmetrical NO stretching frequency constitutes evidence for reduced conjugation with the ring system, whereas the asymmetric NO stretching frequency is insensitive to ortho-effects.³⁹ A comparison of the two spectra shows that the steric and strain effects found in **1** affect not only the vibrational modes of the methyl- and nitro-group but also essentially most fundamentals of these related molecules. One should thus be able to readily distinguish these tautomers from their IR spectrum.⁴⁰

8. Reaction Rates

Since no analytical potential energy surface is available for the reaction considered here, kinetics information cannot be obtained from a molecular dynamics approach. An alternative to molecular dynamics is the “direct” ab initio dynamics approach based on variational transition-state theory (VTST) with semiclassical tunneling corrections.^{41–45} In this work, the canonical VTST technique (CVT) is utilized to obtain the rate constants of the rearrangement of **1** from the geometry, energy, gradient, and Hessian information along the minimum energy path (MEP) of this reaction. For a given temperature, the rate constant is obtained by varying the location of the dividing surface which intersects the reactant and product region of the

(39) Trotter, J. *Canad. J. Chem.* **1959**, *37*, 1487.

(40) Rauhut, G.; Pulay, P. *J. Am. Chem. Soc.* **1995**, *117*, 4167.

(41) Truhlar, D. G.; Garrett, B. C. *Acc. Chem. Res.* **1980**, *13*, 440.

(42) Truhlar, D. G.; Garrett, B. C. *Annu. Rev. Phys. Chem.* **1984**, *35*, 159.

(43) Truhlar, D. G. Direct Dynamics Methods for the Calculation of Reaction Rates. In *The Reaction Path in Chemistry*; Heidrich, D., Ed.; Kluwer: Dordrecht, 1995.

(44) Isaacson, A. D. Using the Reaction Path Concept to Obtain Rate Constants from ab initio Calculations. In *The Reaction Path in Chemistry*; Heidrich, D., Ed.; Kluwer: Dordrecht, 1995.

(45) Truhlar, D. G.; Garrett, B. C.; Klippenstein, S. J. *J. Phys. Chem.* **1996**, *100*, 12771.

(38) Rauhut, G.; Jarzecki, A.; Pulay, P. *J. Comput. Chem.* **1997**, *18*, 489.

Table 6. Experimental and Calculated (B3-LYP/6-31G*) Vibrational Frequencies of 7-Methyl-4-nitrobenzofuroxan (C₈)

no.	sym.	calcd ^a	int. ^b	exptl ^a	assignment
1	a''	51.0	0.4		torsion of nitro-group
2	a''	90.8	0.9		wagging of N ₃ and 6-member ring torsion
3	a''	119.3	1.3		5/6-memb. ring def. and torsion of methyl group
4	a''	130.1	0.1		5/6-memb. ring def. and torsion of methyl group
5	a'	183.3	1.5		C-NO ₂ rocking
6	a''	215.0	0.3		5/6-memb. ring torsion (butterfly)
7	a'	239.4	1.1		C-CH ₃ rocking
8	a''	291.0	0.6		wagging of O ₁ , methyl- and nitro-group
9	a'	331.0	0.5		6-memb. ring def. (C ₃ -C ₆) and N ₃ -C ₆ stretching
10	a''	369.4	5.5		5/6-memb. ring torsion
11	a'	383.0	0.4		5-memb. ring def. and CH-rocking
12	a'	411.0	0.1		rocking of nitro group
13	a'	502.7	1.5		endocycl. NO-stretching
14	a''	508.0	0.1		5/6-memb. ring torsion
15	a''	565.3	0.6		5/6-memb. ring torsion and C-CH ₃ wagging
16	a'	571.4	2.1		5/6-memb. ring def. in plane
17	a''	579.2	1.6		5/6-memb. ring def. torsion and exocycl. NO out-of-plane def.
18	a'	594.2	9.0		6-memb. ring def.
19	a'	685.7	0.6		5/6-memb. ring def. in plane
20	a''	718.8	0.4		5/6-memb. ring torsion
21	a'	729.9	19.8	723.4	5-memb. ring def. and NO ₂ scissoring
22	a''	739.6	19.4	729.4	wagging of nitro group
23	a'	806.3	7.2		5-memb. ring def. (N ₁ -O ₂)
24	a'	815.8	18.8	815.9	NO ₂ scissoring and 6-memb. ring def. in plane
25	a''	852.6	15.2	860.4	H ₁ , H ₂ wagging (symm.)
26	a'	957.6	32.2	966.5	6-memb. ring def. and rocking of methyl group
27	a'	971.6	8.4	976.3	5/6-memb. ring def. and C ₆ -N ₃ stretching
28	a''	985.5	1.5		H ₁ , H ₂ wagging (asymm.)
29	a'	1010.2	28.6	1008.5	5-memb. ring def. and CH ₃ rocking
30	a''	1048.5	5.4	1035.9	rocking of methyl group
31	a'	1106.6	5.4	1105.0	H ₁ , H ₂ rocking (symm.)
32	a'	1116.7	1.5	1123.6	exocyclic stretching of C ₃ -C ₇ and C ₁ -C ₂ , C ₄ -C ₅ stretching
33	a'	1202.0	33.5	1205.7	5/6-memb. ring def. in plane and H ₁ rocking
34	a'	1254.1	2.6		rocking of H ₁ , H ₂ (symm.)
35	a'	1307.4	540.4	1311.8	NO ₂ stretchings and scissoring
36	a'	1325.0	29.8	1325.3	H ₁ , H ₂ rocking and stretching of C ₁ -C ₂ and C ₄ -C ₅
37	a'	1375.8	24.3	1367.7	HCH bendings (symm.) and stretching of C ₂ -C ₃ and C ₁ -N ₁
38	a'	1388.5	1.9	1377.4	rocking of methyl group and 5-memb. ring def.
39	a'	1403.5	37.8	1419.8	5/6-memb. ring def. in plane
40	a''	1439.5	8.9		asymm. CH ₃ def.
41	a'	1454.2	20.7	1456.4	asymm. CH ₃ def.
42	a'	1499.7	1.2	1498.9	stretching of C ₁ -C ₆ and C ₁ -N ₁ and H rocking (symm.)
43	a'	1533.3	159.7	1523.9	NO ₂ stretching (asymm.)
44	a'	1550.1	157.0	1545.2	6-memb. ring def. in plane
45	a'	1587.5	259.8	1581.8	exocyclic N ₂ -O ₁ stretching
46	a'	1618.3	198.3	1620.4	6-memb. ring def. in plane
47	a'	2937.0	2.8		CH stretchings of methyl group (symm.)
48	a''	2991.3	3.3		CH stretchings of methyl group (C ₇ -H ₅ , C ₇ -H ₆)
49	a'	3021.8	13.1		CH stretchings of methyl group (C ₇ -H ₄)
50	a'	3081.6	6.1		C ₄ -H ₂ stretching
51	a'	3111.0	2.8		C ₅ -H ₁ stretching

^a Wavenumber in cm⁻¹. ^b Intensities in km/mol.

potential energy surface of the system along the MEP, to minimize the number of trajectories that are recrossing the reaction barrier from the product to the reactant side of the PES.^{41-43,46} The MEP was computed pointwise at B3-LYP/6-31G** level, using a quadratic steepest descent (QSD) algorithm⁴⁷ as implemented in Molpro.¹⁹ Starting from the tightly optimized saddle point, using a stepsize $s = 0.2 a_0$, the complete MEP was traced out by 30 points. The Hessian was calculated at 12 geometries along the path, selected automatically by the dynamic regeneration scheme of the QSD algorithm. Note that, the Hessians are not calculated at geometries evenly spaced along the reaction path. Instead, the dynamic regeneration scheme of the QSD algorithm automatically selects *dynamically relevant* parts of the reaction path at which the Hessian is calculated. In connection with this dynamic regeneration scheme, the QSD algorithm in combination with the stepsize given above

was found to ensure the accuracy of the required in VTST calculations as has been shown recently.⁴⁷ A correction of the energies of all points calculated along the path with the high level CCSD(T) method was not feasible computationally. However, it was possible to obtain an approximation of the reaction path at the CCSD(T)/6-31G** level using the interpolated VTST method (IVTST1).⁴⁸ This technique attempts to interpolate the reaction path from the geometry, energy, gradient, and Hessian information at the reactant and product minima, the saddle point, and one additional point on the MEP. The additional point was chosen at a distance of $s = 0.1 a_0$ from the saddle point in the direction of the reactant. At each of these geometries, the B3-LYP energy has been corrected by the CCSD(T)/6-31G** values. To test for the importance of recrossing effects, conventional transition-state theory (TST) has also been used to compute the rate constants of the BKR. In (V)TST methodology motion along the reaction path is treated

(46) Truhlar, D. G.; Isaacson, A. D.; Garrett, B. C. Generalized Transition State Theory. In *The Theory of Chemical Reaction Dynamics*; Baer, M., Ed.; CRC Press: Boca Raton, 1985; Vol. 4.

(47) Eckert, F.; Werner, H. J. *Theor. Chem. Acc.* **1998**, *100*, 21.

(48) Gonzales-Lafont, A.; Truong, T. N.; Truhlar, D. G. *J. Phys. Chem.* **1991**, *95*, 8875.

Table 7. Rate Constants for the Boulton–Katritzky Rearrangement of 5-Methyl-4-nitrobenzofuroxan **1**^a

method	B3-LYP	CCSD(T)
TST	8.3×10^{-3}	5.9×10^{-7}
TST/ZCT-0	1.0×10^{-2}	6.7×10^{-7}
IVTST1	8.3×10^{-3}	5.9×10^{-7}
IVTST1/ZCT	9.7×10^{-3}	6.5×10^{-7}
IVTST1/SCT	1.0×10^{-2}	7.3×10^{-7}
CVT	8.1×10^{-3}	
CVT/ZCT	1.1×10^{-2}	
CVT/SCT	1.3×10^{-2}	

^a Rate constants k in 1/s for $T=298$ K. See text for explanation of abbreviations.

classically, while motion transverse to it is treated quantum mechanically. Further quantum effects (i.e., tunneling through the reaction barrier or nonclassical reflection of trajectories at the barrier) were included a posteriori, using some semiclassical correction term (the transmission coefficient) that was multiplied with the (V)TST rate constant. The conventional TST only allows for a one-dimensional adiabatic estimate of the tunneling path, known as zeroth-order or Eckart interpolation zero curvature tunneling (ZCT-0) approximation.⁴⁹ CVT or IVTST1 calculations, where the MEP is known exactly or approximately, also allow for a multidimensional approximation of the tunneling path. The zero curvature tunneling (ZCT) approximation^{50–53} assumes that the tunneling path follows the MEP, whereas the small curvature tunneling (SCT) approximation^{46,54–56} also takes into account “corner-cutting” effects occurring in reaction paths with large curvature. CVT theory in combination with SCT tunneling can be considered the most accurate treatment of the reaction kinetics, regarding the information about the MEP that was available in this work. The reaction rate calculations were done with the program Polyrate.⁵⁷

Table 7 compares the forward rate constants of the BKR of 5-methyl-4-nitrobenzofuroxan for different levels of transition state theory at a temperature of $T = 298$ K. It is obvious that the rate constants depend more critically on the level of theory of the ab initio calculation than on the level of the transition-state theory. The values of the TST, IVTST1, and CVT rate constants at B3-LYP level and their corresponding values at the CCSD(T) level scatter in the usual range, whereas the results at the same level of (V)TST theory differ by several orders of magnitude in dependence on the quantum chemical method. Thus the effect of recrossing trajectories at the reaction barrier can be regarded small. In addition, the semiclassical tunneling corrections did not lead to a substantial increase of the reaction rates. Such a behavior could be expected, since the BKR does not involve hydrogen atoms and tunneling effects can be assumed to be small for atoms heavier than hydrogen. This was

(49) Truong, T. N.; Truhlar, D. G. *J. Chem. Phys.* **1990**, *93*, 1761.

(50) Garrett, B. C.; Truhlar, D. G. *J. Phys. Chem.* **1979**, *83*, 2921.

(51) Garrett, B. C.; Truhlar, D. G.; Grev, R. S.; Magnuson, A. W. *J. Phys. Chem.* **1980**, *84*, 1730.

(52) Garrett, B. C.; Truhlar, D. G.; Grev, R. S. *J. Phys. Chem.* **1980**, *84*, 1749.

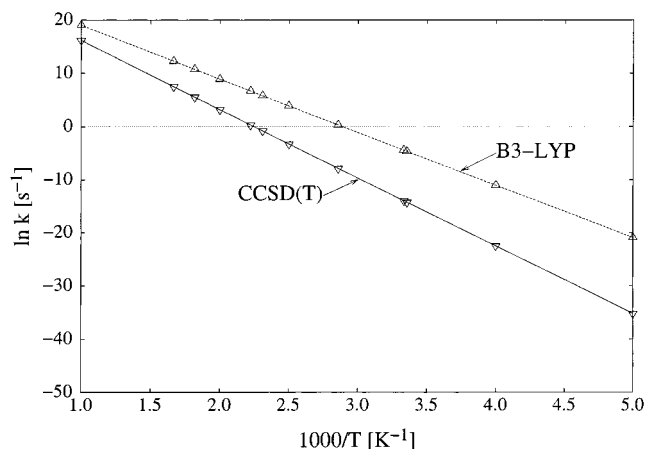
(53) Garrett, B. C.; Truhlar, D. G.; Grev, R. S.; Magnuson, A. W. *J. Phys. Chem.* **1983**, *87*, 4554(E).

(54) Skodje, R. T.; Truhlar, D. G.; Garrett, B. C. *J. Phys. Chem.* **1981**, *85*, 3019.

(55) Skodje, R. T.; Truhlar, D. G.; Garrett, B. C. *J. Chem. Phys.* **1982**, *77*, 5955.

(56) Liu, Y.-P.; Lynch, G. C.; Truong, T. N.; Lu, D.-H.; Truhlar, D. G.; Garrett, B. C. *J. Am. Chem. Soc.* **1993**, *115*, 2408.

(57) Steckler, R.; Chuang, Y.-Y.; Fast, P. L.; Coitiño, E. L.; Corchado, J. C.; Hu, W.-P.; Liu, Y.-P.; Lynch, G. C.; Nguyen, K. A.; Jackels, C. F.; Gu, M. Z.; Rossi, I.; Clayton, S.; Melissas, V. S.; Garret, B. C.; Isaacson, A. D.; Truhlar, D. G. POLYRATE Version 7.3, University of Minnesota, Minneapolis 1997.

**Figure 11.** Arrhenius plot of the rate constants of the Boulton–Katritzky rearrangement of 5-methyl-4-nitrobenzofuroxan **1**.

true even for low temperatures: For a temperature range between 200 and 1500 K, the relative contribution of the semiclassical corrections was always below 40%. Figure 11 shows the Arrhenius plot of the IVTST1/SCT rate constants. Obviously, the reaction is dominated by the exponential term of the TST, i.e., it shows pure Arrhenius behavior. A strong nonclassical contribution to the rate constant would cause deviations from the linearity of the Arrhenius plot at low temperatures. This leads to the conclusion that the magnitude of the rate constant for the BKR of **1** is dominated by the reaction barrier. Consequently, the reaction can be described with sufficient accuracy by the simple transition-state theory.

Thus, the exact determination of the rates does not require knowledge of the complete reaction path, but only of the reaction barrier. However, as can be seen from Table 7, the latter has to be known to a high accuracy and therefore the difference of 5.6 kcal/mol leads to substantial deviations between the B3-LYP and CCSD(T) computed reaction rates. The accuracy of the B3-LYP energies cannot be regarded as sufficient. Energy corrections at CCSD(T) or a similar level of theory are necessary. For instance, as our previous study on unsubstituted 4-nitrobenzofuroxan **5** indicates,⁸ the computationally much less expensive BH&H-LYP density functional theory might be applicable, if dispersion effects are negligible in the considered reaction. The CCSD(T)-energy corrected IVTST1/SCT reaction rates, which can be considered the most reliable, predict a swift reaction at a temperature of about 400 K. Given the exothermicity of the reaction, this confirms the experimental findings, that “on gentle heating” 5-methyl-4-nitrobenzofuroxan **1** completely rearranges to 7-methyl-4-nitrobenzofuroxan **2**.⁶

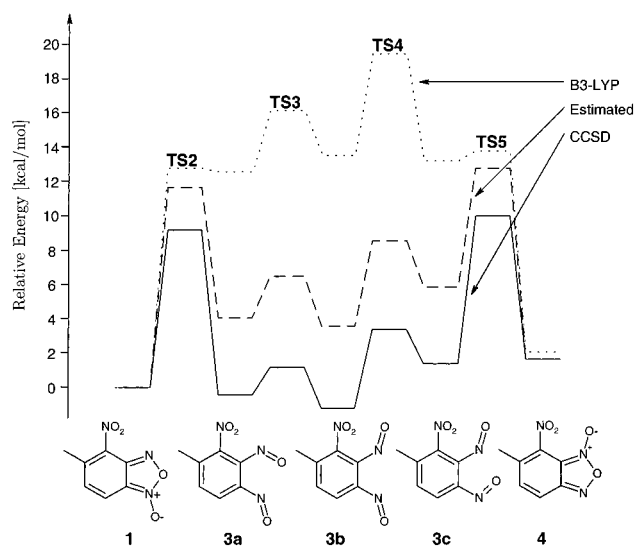
9. Competing Reactions

It is well-known that the ring opening of the heterocyclic ring in benzofuroxans has an activation barrier significantly lower than the one of the BKR. Consequently, the BKR competes in principle with reactions whose first step is the bond cleavage of the endocyclic NO bond. In this sense the most prominent isomeric reaction is the isomerization between 5-methyl-4-nitrobenzofuroxan **1** and 6-methyl-7-nitrobenzofuroxan **4** (Figure 3). The reaction path of this isomerization has been investigated in this study at B3-LYP/6-31G** and CCSD/6-31G** levels and will be compared with high level CCSD(T)/6-31G(2d,p)//MP4(SDQ)/6-31G* calculations for the ring-chain tautomerism of benzofuroxan **7**. For the latter reaction numerous intermediates have been suggested, but computational studies as well as IR and UV experiments by several groups

Table 8. Relative Energies^a of Structures Involved in the Isomerization of 5-Methyl-4-nitrobenzofuroxan **1** toward 6-methyl-7-nitrobenzofuroxan **4**^{b,c}

structure	B3-LYP		CCSD		estimated ^b	
	E_{rel}	E_{rel}^{scal}	E_{rel}	E_{rel}^{scal}	E_{rel}	E_{rel}^{scal}
TS2	14.75	12.83	11.16	9.24	13.5	11.5
3a	14.65	12.55	1.67	-0.43	6.2	4.1
TS3	18.49	16.12	3.63	1.26	8.8	6.5
3b	16.17	13.63	1.39	-1.16	6.2	3.6
TS4	22.30	19.50	5.77	3.40	11.0	8.6
3c	15.40	13.27	3.52	1.38	8.0	5.9
TS5	15.80	13.76	11.61	9.76	13.9	12.1
4	2.36	2.07	1.96	1.67	2.0	1.7

^a Notation and parameters as in Table 2. Absolute energies and zero-point vibrational energies (ZPE) for all calculations presented in this table are provided in the Supporting Information section of this journal. ^b Estimated CCSD(T) values; for explanation see text. ^c Geometries were optimized at B3-LYP/6-31G** level. Energies refer to the 6-31G** basis also.

**Figure 12.** Reaction path and energy profile of the isomerization of 5-methyl-4-nitrobenzofuroxan **1** toward 6-methyl-7-nitrobenzofuroxan **4**. Relative energies of all structures are shown in Table 8.

showed that 1,2-dinitrosobenzene is the only intermediate relevant to this reaction.^{58–62} Relative energies for the generation of **4** and the ring-chain tautomerism of **7** are provided in Tables 8 and 9. An energy profile for the reaction of **1** is shown in Figure 12.

It was shown recently that the relative energy of the transition state of the furoxan ring opening depends strongly on the quality of the wave function.⁸ Even the relative energies of the intermediate dinitrosobenzene conformers show a strong dependence on the level of computation. This makes the investigation of these reactions rather tedious. Therefore, the model reaction of the tautomerism of benzofuroxan **7** (see Figure 13) has been investigated at the very high CCSD(T)/6-31G(2d,p)//MP4(SDQ)/6-31G* level which due to its high computational requirements was not applicable to the competing reaction shown in Figure 3. However, conclusions drawn for this model reaction can be transferred and thus allow for a better interpretation of the corresponding reaction of **1**. The model reaction was

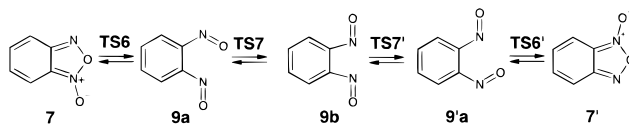
(58) Ponder, M.; Fowler, J. E.; Schaefer, H. F. *J. Org. Chem.* **1994**, *59*, 6431.

(59) Hacker, N. *J. Org. Chem.* **1991**, *56*, 5216.

(60) Dunkin, I.; Lynch, M.; Boulton, A.; Henderson, N. *J. Chem. Soc., Chem. Commun.* **1991**, 1178.

(61) Murata, S.; Tomioka, H. *Chem. Lett.* **1992**, 57.

(62) Igel-Mann, G.; Stoll, H.; Preuss, H. *Mol. Phys.* **1988**, *65*, 1321.

**Figure 13.** Ring-chain tautomerism of benzofuroxan **7**.**Table 9.** Relative Energies^a of Structures Involved in the Ring-Chain Tautomerism of Benzofuroxan^{b,c}

Structure	CCSD		CCSD(T)	
	E_{rel}	E_{rel}^{scal}	E_{rel}	E_{rel}^{scal}
TS6	18.31	16.80	13.33	11.81
9a	1.98	0.35	6.61	4.97
TS7	5.16	3.02	10.34	8.20
9b	0.71	-1.15	5.47	3.61

^a Notation and parameters as in Table 2. Absolute energies for all calculations presented in this table are provided in the supporting information section of this journal. ^b Estimated CCSD(T) values; for explanation see text. ^c Geometries were optimized at MP4(SDQ)/6-31G* Level. Energies refer to the 6-31G(2d,p) basis.

investigated at the B3-LYP level in ref 16. At this level the rotations of the nitroso-groups are the rate determining steps. In contrast, it is the bond cleavage of the endocyclic NO bond that determines the reaction at the CCSD and CCSD(T) levels. As discussed previously, CCSD(T) energies must be considered superior to B3-LYP calculations, but as shown above B3-LYP geometries for equilibrium structures are reliable. Unfortunately, the triples correction has significant impact on the relative stability of the dinitroso compounds **9** as can be seen in Table 9. On the basis of experimental evidence (i.e., benzofuroxan is more stable than dinitrosobenzene) CCSD energies do not correctly describe the energetics of this reaction. However, the triples correction, which lowers the rate-determining transition state by about -5.0 kcal/mol and shifts all dinitrosobenzene structures by about the same amount in the opposite direction, consequently leads to results which are in good agreement with experimental findings.

The same difference between CCSD and B3-LYP calculations can also be found for the isomerization of **1** toward **4**. Moreover, two structures at the CCSD level are lower in energy than the educt indicating again that the connected triples correction is mandatory (even though it could not be applied here) for these molecules. On the basis of the knowledge of the model reaction we therefore have estimated the triples contribution to yield approximate CCSD(T) energies. These values are shown in Table 8. Unfortunately, it was necessary to apply another correction to the transition state that corresponds to the bond cleavage in **1**. The structure of this transition state is shown in Figure 14. We were able to show recently that B3-LYP is not able to predict the corresponding structure as involved in the rearrangement of unsubstituted 4-nitrobenzofuroxan entirely correct. Therefore, on the basis of our study of the BKR of 4-nitrobenzofuroxan **5** the energy difference arising from the difference between the more reliable MP4(SDQ) structure and the B3-LYP structure can be estimated to be about 7.3 kcal/mol. This correction overcompensates for the triples correction, and thus the transition state of the ring opening is corrected in the same direction as that for the dinitrosobenzene structures. This additional correction was taken into account in Table 8. We emphasize here that due to these estimations the provided energies for this alternative reaction must be considered less reliable and must be seen qualitatively rather than quantitatively.

All transition states involved in this mechanism lie well below the activation barrier of the BKR, and thus this reaction may be observed at temperatures lower than that for the BKR. Note

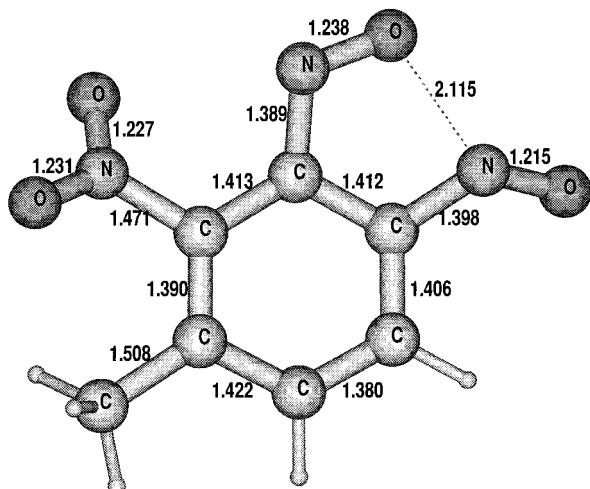


Figure 14. Structure of the transition state of the ring chain isomerization of **1** (B3-LYP/6-31G**).

that, the relative energy of **4** most likely is not going to change upon the inclusion of triple excitations (only the dinitrosobenzene structures are affected) and is thus only 1.7 kcal/mol less stable than **1**.

An analogous reaction can, of course, be formulated for the isomerization of the 7-methyl isomer, but this reaction will be even less favorable due to the stabilizing interaction between the methyl-group and the exocyclic oxygen atom.

10. Summary and Conclusions

The Boulton–Katritzky rearrangement of 5-methyl-4-nitrobenzofuroxan **1** was investigated by using quantum chemical and experimental methods. The reaction barrier of about 26 kcal/

mol is significantly higher than the barrier of the isomerization toward 6-methyl-7-nitrobenzofuroxan **4**. However, the first reaction is exothermic by about 4 kcal/mol, while the latter is endothermic by about 2 kcal/mol. An energy partitioning identifies the dominant driving forces for this BKR to be strain effects of the six-membered ring as well as electronic (anti-conjugative) effects due to the out-of-plane torsion of the nitro-group. Both effects must be considered secondary effects since they originate from steric hindrance of the methyl-group in the ortho-position to the nitro-group. Positive inductive effects appear to accelerate the reaction as well but this contribution could not safely be quantized. Strain and anti-conjugative effects are essentially active in all 5-substituted 4-nitrobenzofuroxans (see the exception of 5-cyano-4-nitrobenzofuroxan in Table 5) but mesomeric effects appear to have significant impact as well. O···H interactions accelerate the reaction of 5-methyl-4-nitrobenzofuroxan but may have the opposite effect when forming true hydrogen bonds.

Acknowledgment. Computer time on the SGI PowerChallenge of the Institut für Theoretische Chemie (Stuttgart) and on the NEC SX-4 of the High-Performance Computing Center for Science and Industry (Stuttgart) is kindly acknowledged. We thank Prof. D. G. Truhlar for providing us with a copy of the program Polyrate and G. Hetzer for valuable discussions.

Supporting Information Available: Tables of absolute energies and zero-point vibrational energies for all stationary points, tables of crystal data, structure solution and refinement, atomic coordinates, bond lengths and angles, anisotropic displacement parameters, and natural internal coordinates for **2**, and vibrational assignments for **1** (PDF). This material is available free of charge via the Internet at <http://pubs.acs.org>.

JA990475U